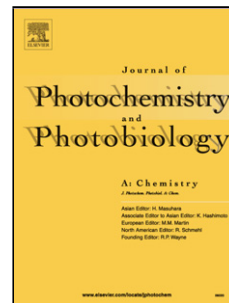


Accepted Manuscript

Title: Styrylcyanine-based fluorescent probes with red-emission and large Stokes shift for the detection of viscosity

Authors: Xiangbin Cao, Jianhui Liu, Pan Hong, Guanglan Li, Ce Hao



PII: S1010-6030(17)30259-9
DOI: <http://dx.doi.org/doi:10.1016/j.jphotochem.2017.05.035>
Reference: JPC 10662

To appear in: *Journal of Photochemistry and Photobiology A: Chemistry*

Received date: 25-2-2017
Revised date: 19-4-2017
Accepted date: 22-5-2017

Please cite this article as: Xiangbin Cao, Jianhui Liu, Pan Hong, Guanglan Li, Ce Hao, Styrylcyanine-based fluorescent probes with red-emission and large Stokes shift for the detection of viscosity, *Journal of Photochemistry and Photobiology A: Chemistry* <http://dx.doi.org/10.1016/j.jphotochem.2017.05.035>

This is a PDF file of an unedited manuscript that has been accepted for publication. As a service to our customers we are providing this early version of the manuscript. The manuscript will undergo copyediting, typesetting, and review of the resulting proof before it is published in its final form. Please note that during the production process errors may be discovered which could affect the content, and all legal disclaimers that apply to the journal pertain.

Styrylcyanine-based fluorescent probes with red-emission and large Stokes shift for the detection of viscosity

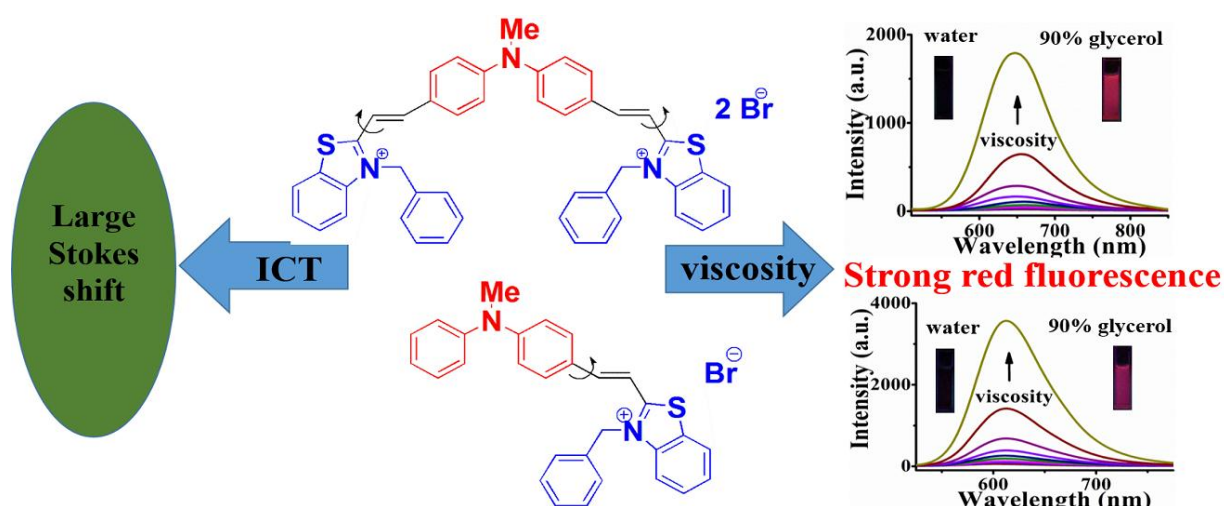
Xiangbin Cao, Jianhui Liu*, Pan Hong, Guanglan Li and Ce Hao*

School of Petroleum and Chemical Engineering, Dalian University of Technology, Panjin, Liaoning 124221, P. R. China

* Corresponding author: liujh@dlut.edu.cn (J. Liu)

haoce@dlut.edu.cn (C. Hao)

Graphical Abstract



Highlights

- Two novel styrylcyanine dyes were developed based on ICT.
- The probes exhibited red-emission and large Stokes shift.
- The probes displayed high sensitivity to viscosity.
- The fluorescence intensity was affected by intramolecular rotation.

Abstract: Based on the mechanism of intramolecular charge transfer (ICT), two new styrylcyanine dyes, **DPA-1** and **DPA-2**, composed of an electron-rich *N*-phenylaniline and a cationic benzothiazene connected with ethylene(s) bridge, were designed and synthesized. These two dyes exhibited red-emission (653/607 nm) and simultaneously impressive large Stokes shift (111/92 nm) due to intramolecular charge transfer effect, twisted geometry and extended conjugation system. When their solution viscosity increased from 1.01 cP to 234 cP in the water-glycerol system, the fluorescence

intensity of the synthetic dyes was enhanced by 81-fold and 64-fold, respectively. Additionally, a favorable linear relationship between the fluorescence intensity and the environmental viscosity was observed within the above viscosity range for the obtained samples ($R^2 > 0.99$), which led to the establishment of a method for the quantitative determination of the solution viscosity. Such dyes with improved photophysical properties, including emission wavelength and Stokes shift, could be used as promising candidates for intracellular viscosity detection. Moreover, the mechanism of fluorescence emission of the resultant products toward viscosity was further investigated. Of the two probes studies, **DPA-1** is better than **DPA-2** in terms of emission wavelength, Stokes shift and the sensitivity of the fluorescence intensity to viscosity.

Keywords: red-emission; large Stokes shift; styrylcyanine; viscosity; intramolecular charge transfer

1. Introduction

Diffusion-mediated cellular processes, including transportation of mass and signal, interactions between biomolecules and diffusion of reactive metabolites, can be influenced by intracellular viscosity [1,2]. Indeed, abnormal changes in viscosity are connected to a wide range of diseases and dysfunctions [3], such as atherosclerosis and diabetes [4,5]. Therefore, the detection of intracellular viscosity is important for biological analysis and disease diagnosis [6].

Fluorescent molecular rotors are good candidates to be used for determining the viscosity of a microenvironment [2]. These fluorescent molecules can freely rotate in low-viscosity media, resulting in the weak intrinsic fluorescence. Once the intramolecular rotation is restricted in viscous media, the fluorescence intensity or lifetime of the dyes will increase [7-10]. To date, various kinds of molecular rotors have been used to make great achievements in intracellular viscosity research. However, traditional molecular rotors are limited to 9-(dicyanovinyl)-julolidine (**DCVJ**) and their derivatives [7,8,11]. Porphyrin-based rotors suffer from complicated synthesis and low sensitivity [1,12]. The applications of BODIPY-based rotors [10,13-16] for *in vivo* analysis may be limited by their short wavelength, due to the significant auto-fluorescence of biomolecules by excitation with visible light [17,18]. On the other hand, the cyanine dyes have been used as chemosensors for intracellular viscosity detection due to their perfect photophysical properties and outstanding biocompatibility [2,3,19-23]. For instance, Peng et al. reported a

pentamethine cyanine dye **RY3** with a formyl group as the rotor to determine the intracellular viscosity [2]. Moreover, Belfield et al. [24] reported two near-infrared viscosity probes based on squaraine, where biomolecules exhibit the least absorption and auto-fluorescence background [8,25]. However, the small Stokes shift of cyanine dyes can cause the self-quenching and influence the accuracy of the measurement, due to the significant overlap of the absorption and emission spectra from the probes [8,25,26]. Thus, it is urgent to design a red-shifted emission fluorescent probe with large Stokes shift for the determination of intracellular viscosity.

Generally, the emission wavelengths of the dyes can be increased by introducing a conjugated vinyl group as reported by Telore and Peng [27,28]. Also, some studies have shown that the large Stokes shift can be usually achieved by the intramolecular charge transfer (ICT) effect [25,29,30]. Benzothiazene is often chosen as the acceptor (**A**) moiety due to its excellent ICT structures and outstanding photophysical performances [27,31-34]. In this study, *N*-methyldiphenylamine was used as the donor (**D**) moiety, as they have been employed as hole-transporting materials inorganic light-emitting diodes (OLED) [35]. The acceptor and donor moieties were connected by ethylene, which enables to extend the conjugation system, hence releasing the longer wavelength fluorescence [36,37]. Based on this consideration, we anticipated that the resulting dyes would simultaneously achieve large Stokes shift and red-emission. We also postulate that the obtained samples could be used for microviscosity detection owing to the presence of several rotatable C-C bonds according to previous reports [21,23]. In addition, the rotation of chemical bonds increases the flexibility of the molecular skeleton, and thus increases the Stokes shift, which has been reported by some researchers [8,28]. In this study, two new styrylcyanine dyes (**DPA-1** and **DPA-2**) based on ICT principle were constructed by the ethylene bridged *N*-methyldiphenylamine and benzothiazene (Scheme 1). The relationship between the fluorescence and the viscosity was also further investigated.

2. Experimental section

2.1. Materials and instruments

All the solvents and reagents were obtained from commercial suppliers and used directly without any further purification. All reactions were carried out with agitation using a magnetic stirrer. The NMR spectra were recorded with a Bruker Avance 500 MHz instrument, using tetramethylsilane (TMS) as an internal standard. Mass spectrometry (MS) was performed on Q-TOF-MS instruments. UV-Vis absorption

spectra were recorded with an Agilent Carry 60 spectrophotometer. The target dye molecules were dissolved in dimethyl sulfoxide (DMSO) to produce 1 mM of stock solutions. Fluorescence spectroscopy was conducted with a F97Pro spectrophotometer (Shanghai Lengguang Technology Co., Ltd., Shanghai, China). The fluorescence intensity was adjusted to a suitable range by modifying the excitation and emission slit widths. **DPA-1** and **DPA-2** were excited at 470 nm and 490 nm, respectively.

2.2. Synthesis of **DPA-1**

The thiazole-based quaternary ammonium salt **4** and other intermediates (**3a** and **3b**) were synthesized according to published procedures [35,38,39]. Benzothiazolium bromide salt **4** (0.64 g, 2.0 mmol) and the diformylated derivative **3a** (0.06 g, 0.25 mmol) were mixed in 10 mL of anhydrous ethanol and a catalytic amount of pyridine (0.1 ml) was added. The reaction mixture was refluxed under nitrogen for 48 h, and then filtered *in vacuo*. The crude solid product was further purified by recrystallization in ethanol. The yield was 94%.

¹H NMR (500 MHz, DMSO-*d*₆), δ (ppm): 8.44 (dd, *J* = 8.0, 1.4 Hz, 2H), 8.30 (d, *J* = 15.5 Hz, 2H), 8.17-8.12 (m, 2H), 8.09-8.04 (m, 4H), 8.03 (d, *J* = 2.0 Hz, 2H), 7.80 (ddd, *J* = 8.5, 7.3, 1.5 Hz, 2H), 7.78-7.74 (m, 2H), 7.43-7.37 (m, 4H), 7.37-7.33 (m, 6H), 7.33-7.28 (m, 4H), 6.25 (s, 4H), 3.52 (s, 3H). ¹³C NMR (126 MHz, DMSO-*d*₆), δ (ppm): 173.2, 151.0, 150.1, 141.7, 134.5, 132.5, 130.0, 129.6, 128.9, 128.8, 128.4, 128.2, 127.4, 125.0, 121.1, 117.2, 111.1, 51.7, 39.6. MS (ESI): *m/z* calcd: for C₄₅H₃₇Br₂N₃S₂ 341.6212 [M - 2Br]²⁺; found: 341.6209.

2.3. Synthesis of **DPA-2**

DPA-2 was prepared in a similar manner as described for **DPA-1**. The yield was 88%.

¹H NMR (500 MHz, DMSO-*d*₆), δ (ppm): 8.38 (dd, *J* = 8.1, 1.3 Hz, 1H), 8.20 (d, *J* = 15.2 Hz, 1H), 8.11-8.02 (m, 1H), 7.92-7.87 (m, 2H), 7.84 (d, *J* = 15.3 Hz, 1H), 7.75 (ddd, *J* = 8.5, 7.2, 1.3 Hz, 1H), 7.70 (ddd, *J* = 8.2, 7.2, 1.1 Hz, 1H), 7.53-7.46 (m, 2H), 7.41-7.36 (m, 2H), 7.36-7.29 (m, 6H), 6.87-6.82 (m, 2H), 6.17 (s, 2H), 3.41 (s, 3H). ¹³C NMR (126 MHz, DMSO-*d*₆), δ (ppm): 172.8, 153.1, 151.2, 146.6, 141.7, 134.6, 133.1, 130.5, 129.7, 129.6, 128.9, 128.3, 127.8, 127.3, 126.8, 126.6, 124.7, 123.8, 116.8, 114.6, 107.9, 51.3, 40.8. MS (ESI): *m/z* calcd: for C₂₉H₂₅BrN₂S 433.1733 [M - Br]⁺; found: 433.1747.

2.4. Fluorescence quantum yield measurements

The relative fluorescence quantum yield was determined according to the following equation [40]:

$$\Phi_x = \Phi_s(F_x/F_s)(A_s/A_x)(\lambda_s/\lambda_x)(n_x/n_s)$$

Where, Φ is the quantum yield, F is the integrated area under the corrected emission spectrum, A is absorbance at the excitation wavelength, λ is the excitation wavelength, n denotes the refractive index of the solution (since the concentrations of the solutions is very low, ranging from 10^{-7} - 10^{-8} mol/L, the refractive indices of the solutions were replaced with those of the solvents), and the subscripts x and s refer to the unknown and the standard, respectively. Here, rhodamine B ($\Phi_F = 0.97$ in ethanol) was used as the reference standard.

2.5. Viscosity and fluorescence spectral measurement

The solvents were prepared by mixing deionized water-glycerol systems in different proportions. The viscosity was recorded using a rotational viscometer (NDJ-5S, Shanghai Hengping Scientific Instrument Co., Ltd., Shanghai, China). A 100 μ L volume of stock solution (1.0 mM in DMSO) was added to the water-glycerol mixture (10 mL) to give a final concentration of 10.0 μ M. The air bubbles in these solutions were removed by sonicating for 30 min. The solution was kept for one hour at a constant temperature (20°C), then the absorption and emission spectra were measured in a UV-Vis spectrophotometer and a fluorescence spectrophotometer, respectively.

The quantitative relationship between fluorescence intensity and the viscosity of solvent was fitted by the Förster-Hoffmann equation as follows [41]:

$$\log I_f = C + x \log \eta$$

Where, I_f stands for the fluorescence intensity, C represents the constant related to probe concentration and temperature, x is the probe-dependent constant and η denotes the viscosity of the solvent.

2.6. Low temperature fluorescence spectra

The fluorescence intensity of the probes was measured in a glycerol/water (7:3, v/v) mixture (10.0 μ M) at 0, 5, 15, 20, 25, 35 and 40°C at the corresponding excitation wavelength.

2.7. Fabrication of PMMA films

An 80 μL volume of stock solution was added to 400 μL of CH_2Cl_2 containing 14.0 mg of polymethylmethacrylate (PMMA). Then, the resulting mixture was coated onto the surface of a thin quartz plate (2.5 cm diameter). The solvent was then allowed to evaporate.

2.8. Computational study

All the calculations of geometry optimizations of the dyes were carried out using density functional theory (DFT) and time-dependent density functional theory (TDDFT) in the Gaussian 09 software package [42]. The B3LYP functional [43] and 6-31G* basis set [44] were used to calculate the geometry optimization and scan the potential energy curves in both S_0 state and S_1 state. Based on the optimized geometry, we calculated the absorption spectrum in the level of PBE0/6-311G* [45,46] with the method of IEFPCM model in water. Additionally, the potential-energy curves of the ground state (S_0) were qualitatively scanned by constrained optimizations, keeping the dihedral angles fixed at a series of values. The potential energy curves of S_1 were obtained in a similar manner as described for S_0 using the TDDFT method.

3. Results and Discussion

3.1. Design and synthesis of the *DPA-1* and *DPA-2*

As mentioned above, *N*-methyldiphenylamine has been employed as a hole-transporting material in OLED [35], and therefore it was chosen as the donor part in our studies. As for acceptor unit, benzothiazene was chosen due to its electron-deficient property, enabling to have a better effect to accept the incoming electrons. In addition, benzothiazene tends to construct ICT structures and achieve excellent photophysical performances [27,31,32]. Overall, this kind of donor- π -bridge-acceptor (**D- π -A**) provides them with large conjugated system and strong ICT effect, and this will be beneficial for the attainment of a large Stokes shift and a long wavelength emission [25,33]. Moreover, the quaternized aromatic amino groups endow the probes with good water solubility, while the benzyl group introduced further regulates lipid solubility [3] and helps it to accumulate in mitochondria [33]. In addition, we anticipated that **DPA-1** and **DPA-2** would be used for microviscosity detection due to the presence of several rotatable C-C bonds on these two molecules [21,23].

The synthetic route was designed for our two DPA analogues in four steps, starting from commercially available diphenylamine (**1**), which can be methylated to

obtain *N*-methyldiphenylamine (**2**) via nucleophilic substitution with iodomethane. Then, it was formylated by the Vilsmeier-Haack reaction to obtain the required intermediates, **3a** and **3b**, according to the previously reported literature. The thiazole-based quaternary ammonium salt (**4**) was synthesized by mixing 2-methyl benzothiazole and benzyl bromide in the absence of solvent at 110°C for 3 h with excellent yield (96%). The ammonium salt **4** (1 eq.) was heated with **3a** (0.125 eq.) in the presence of a catalyzed amount of pyridine to give one of the final products, **DPA-1**, by Knoevenagel condensation. The analogue **DPA-2** was obtained in a similar way by the reaction of **4** with excess of **3b** (0.25 eq.). The crude products were purified by recrystallization and characterized by ¹H NMR, ¹³C NMR and MS.

3.2. Spectral properties of **DPA-1**

To characterize the spectral properties of the sensors, we first studied the solvent dependency of **DPA-1**. It can be observed from data shown in Table S1 that the maximum emission wavelength varied substantially with the polarity of the solvents (dichloromethane, THF, acetonitrile, DMSO and water), while little change was observed in the maximum absorption (around 542 nm), which further indicated the occurrence of the ICT effect on **DPA-1** as reported by Wang and Fan [33,47]. As anticipated, **DPA-1** exhibits an absorption maximum (λ_{abs}) at 542 nm and an emission maximum (λ_{em}) at 653 nm (Fig. 1) in water, which are greatly red-shifted compared with the reported rotor **DCVG** ($\lambda_{\text{em}} = 502$ nm). This result may be attributed to the extended conjugation system of **DPA-1**. Moreover, it exhibits a notably larger Stokes shift (111 nm) than that of **DCVG** (42 nm), which may be ascribed to the ICT effect and the twisted geometry. These intriguing photophysical properties make them suitable candidates for biological analysis. These intriguing photophysical properties make them suitable candidates for biological analysis. It should be noted that **DPA-1** shows quite low fluorescence quantum yield in these solvents possibly because the excited dye releases substantial energy by non-radiative deactivation, and therefore results in weak fluorescence [27,48]. In addition, the fluorescence response of **DPA-1** to a narrow polarity range with different proportions of water and 1, 4-dioxane was evaluated. The evaluation revealed that when the solvent polarity decreases by adding 1, 4-dioxane to water, **DPA-1** shows small responses by a 6.7-fold fluorescence enhancement, as shown in Fig. 2. This result indicates that polarity changes have little interference in the fluorescence intensity of **DPA-1**, which is consistent with previous report [3].

3.3. Fluorescence response to solvent viscosity

Unlike its lower response to polarity, **DPA-1** showed significant fluorescence enhancement upon changes of solution viscosity. The viscous media with different viscosity could be obtained by mixing glycerol and water at different volume ratio. As the viscosity of the solution increased from 1.01 cP in water to 234 cP in 90% of glycerol, the fluorescence intensity of **DPA-1** at 650 nm was substantially increased by 81-fold (Fig. 3a). We consider this result to be promising because this is attributed to viscosity-dependent rotation between *N*-methyldiphenylamine and benzothiazene (Scheme 2). Such rotation is restricted in the presence of viscous solution, i.e., this rotation is negatively correlated with viscosity. In this case, the energy of the excited state is reserved for emission without non-radiative energy dissipation throughout the rotation [15,23]. Meanwhile, no apparent changes were observed in absorption of **DPA-1** with the changes of solution viscosity, which indicated that the molecular structure of the probe remained unaltered [21].

As illustrated in Fig. 3b, **DPA-1** fits the Förster–Hoffmann linear relationship between the fluorescence intensity ($\log I_{650}$) and the viscosity ($\log \eta$) ($R^2 = 0.998$, $x = 0.814$). This linear correlation is crucial and provided a reliable option for **DPA-1** to be employed to detect the viscosity in various media. Also, the presence of some additives, like cysteine (Cys), glutathione (GSH), Fe^{3+} and Cu^{2+} , had no obvious influence on the fluorescence at 650 nm for **DPA-1** (Fig. 4). This better selectivity of **DPA-1** to viscosity over some other substances suggested that they had experienced no interference in the fluorescence intensity at 650 nm as reported by Wang [23].

3.4. Low temperature fluorescence spectra

The relation between fluorescence intensity and the temperature was also examined. As the temperature decreased from 40°C to 0°C, the fluorescence intensity of **DPA-1** at 650 nm was enhanced by 3-fold, although no wave-shift were observed in the fluorescence spectra (Fig. 5a). This indicated that the decrease of temperature can effectively restrain the intramolecular rotation between *N*-methyldiphenylamine and benzothiazene in the **DPA-1**, and thus resulted in the enhancement of the fluorescence, which is consistent with the literature [2,20]. Moreover, a good linear relationship was observed between $\log (I_{650})$ and temperature (Fig. 5b), which is expected since the viscosity is inversely proportional to the temperature, according to “Andrade’s equation”.

3.5. Emission spectrum of **DPA-1** in solid state

To further verify the hypothesis of free intramolecular rotation, the solid-state emission of **DPA-1** was investigated. As previously stated, the free intramolecular rotation is suppressed with the increase of the viscosity of the solution, thus favoring fluorescence. In contrast to the situation in 90% glycerol, **DPA-1** in the PMMA film displayed stronger fluorescence (Fig. 6). This result indicated that intramolecular rotation cannot be completely restricted by glycerol, and on the contrary, rigid environment of the solid state is able to restrict non-radiative deactivation induced by free rotation of **DPA-1** to a greater degree, hence releasing more intense fluorescence [49]. Meanwhile, it is noteworthy that the maximal emission wavelength of **DPA-1** in the PMMA film is slightly blue-shifted compared with the situation in 90% glycerol, which may be ascribed to the aggregation of the dyes molecules [49,50].

3.6. Photophysical and sensing properties of **DPA-2**

Similarly, the spectral properties of **DPA-2** were also investigated (Fig. S2-S8 and Table S2). Compared with its **DPA-1** analogue, in water, **DPA-2** displayed a blue-shifted absorption at 515 nm and an emission wavelength at 607 nm (Fig. S2). This may be ascribed to its larger conjugate structure due to an additional benzothiazene, which would provide a strategy for the design of new red-shifted emission probes. A larger quantum yield ($\Phi_F = 0.009$) was observed from **DPA-2** compared to that of **DPA-1** ($\Phi_F = 0.005$), probably due to the less deactivation of its pathway (Scheme 2). Furthermore, **DPA-2** exhibited a lower viscosity sensitivity (64-fold) compared to that of **DPA-1** (81-fold). This phenomenon may apparently be attributed to its larger quantum yield. The reduction of the intrinsic fluorescence quantum yields is beneficial to improve the environmental sensitivity of the viscosity probes, which is consistent with the literature [48].

To further investigate the corresponding photophysical and sensing properties, we compared our probes with those of other previously reported studies as list in Table S3. Compared with these viscosity probes, such as **RY3** and **dA-SQ**, the obvious advantage of our products is that they display a larger Stokes shift (> 90 nm), which can be attributed to the ICT effect and the twisted geometry. In addition to this, it is noteworthy that the dyes developed by us exhibited red emission and large Stokes shift simultaneously, which may effectively avoid the influence of auto-fluorescence and self-quenching during *in vivo* analysis [25]. Moreover, as can be seen from the Table S3, the fluorescence intensity of the synthesized dyes exhibit comparable or

outperform the sensitivity to solution viscosity (81-fold and 64-fold), which benefits measurement accuracy. Therefore, these intriguing properties make them suitable candidates for measurement of intracellular viscosity.

3.7. Theoretical calculations

To gain a better insight into the molecular geometries and absorption spectra, we performed theoretical calculations in the framework of the DFT and TDDFT methods. The highest occupied molecular orbital (HOMO) of **DPA-1** is mainly located on the *N*-methyldiphenylamino group and the lowest unoccupied molecular orbital (LUMO) on the benzothiazanyl moiety, indicating the electron density transfer from the electron-rich *N*-methyldiphenylamino group to the electron-poor benzothiazanyl moiety, as shown in Fig. 7. This is characteristic of the ICT [48]. The transition (HOMO \rightarrow LUMO) of the **DPA-2** also involves an ICT process, however the charge transfer is smaller than that of **DPA-1**. Moreover, according to our calculations, the energy difference from **DPA-1** (2.26 eV) is smaller than that of **DPA-2** (2.60 eV), leading to a blue-shift in the electronic spectra of **DPA-2** compared to **DPA-1**. The result is in line with the above experimental results of the study on absorption spectra, which indicates that our theoretical calculations are reliable for this study.

Moreover, the mainly non-radiative deactivation of the synthesized probes was further investigated based on the DFT/TDDFT. According to the literature [23,48,51,52], the low quantum yield is mainly caused by the non-radiative deactivation in the excited state, which may be ascribed to rotation of the methine chain. The main non-radiative deactivation occurs in the single excited state with a remarkably low energy gap to the ground state, which is formed during the rotation of the methine chain [48,53]. As illustrated in Scheme 3, several C-C bonds are involved in the rotation (vinyl double bond is negligible because of significant structure overlap during the rotation and only one side of **DPA-1** is considered to simplify the computational processes). The quantum chemical calculations based on the DFT/TDDFT could explain which chemical bond dominates the non-radiative deactivation [23,48]. The potential energy curves of the resultant products in the S_0 and S_1 states with different torsion dihedral angles are qualitatively scanned (Fig. 8, S10). The activation energy and energy gap for rotations around different C-C bonds of the resulting dyes in the S_0 and S_1 states are calculated. As listed in Table 1, the result indicated that rotation about φ_1 is more difficult than that about φ_2 for the **DPA-1** because of the higher rotational energy barrier in the excited state and the larger

energy gap to the ground state. Accordingly, the rotation of the chemical bond close to benzothiazene (φ_2) should be responsible for the mainly non-radiative deactivation of **DPA-1**. However, the results of the calculation of the activation energy and energy gap for **DPA-2** suggested that the non-radiative deactivation was dominated by the rotation of the chemical bond close to *N*-methyldiphenylamine (φ_1). The rotation of different chemical bonds causes mainly non-radiative deactivation for the two analogues, which may be associated with molecular symmetry [48]. In addition, **DPA-2** showed higher intrinsic fluorescence quantum yield than **DPA-1**, due to a higher rotating energy barrier. The result is consistent with the experimental results. Of the two synthetic probes, **DPA-1** demonstrated higher sensitivity (81-fold) toward viscosity than **DPA-2** (64-fold), due to its lower quantum yield.

4. Conclusions

In conclusion, we have developed two novel styrylcyanine dyes based on ICT and confirmed their usefulness as fluorescent probes. Our synthetic dyes exhibited larger Stokes shift derived from, the strong ICT effect and twisted geometry, and red-emission from the extended conjugation system. The obtained samples also showed remarkable fluorescence enhancement on increasing the environmental viscosity due to the restrain of intramolecular rotation. Their larger Stokes shift and red-emission give them the potential for biological analysis. Meanwhile, a linear relationship between the fluorescence intensity and the environmental viscosity could be used for quantitative determination of microviscosity.

Acknowledgements

This work has been supported by the National Natural Science Foundation of China (Grant Nos. 21373042 and 21677029).

References

- [1] M. K. Kuimova, S. W. Botchway, A. W. Parker, M. Balaz, H. A. Collins, H. L. Anderson, K. Suhling, P. R. Ogilby, Imaging intracellular viscosity of a single cell during photoinduced cell death, *Nat. Chem.* 1 (2009) 69-73.
- [2] X. Peng, Z. Yang, J. Wang, J. Fan, Y. He, F. Song, B. Wang, S. Sun, J. Qu, J. Qi, M. Yan, Fluorescence ratiometry and fluorescence lifetime imaging: using a single molecular sensor for dual mode imaging of cellular viscosity, *J. Am. Chem. Soc.* 133 (2011) 6626-6635.
- [3] N. Jiang, J. Fan, S. Zhang, T. Wu, J. Wang, P. Gao, J. Qu, F. Zhou, X. Peng, Dual mode monitoring probe for mitochondrial viscosity in single cell, *Sensors Actuators B: Chem.* 190 (2014) 685-693.
- [4] G. Deliconstantinos, V. Villiotou, J. C. Stavrides, Modulation of particulate nitric-oxide synthase

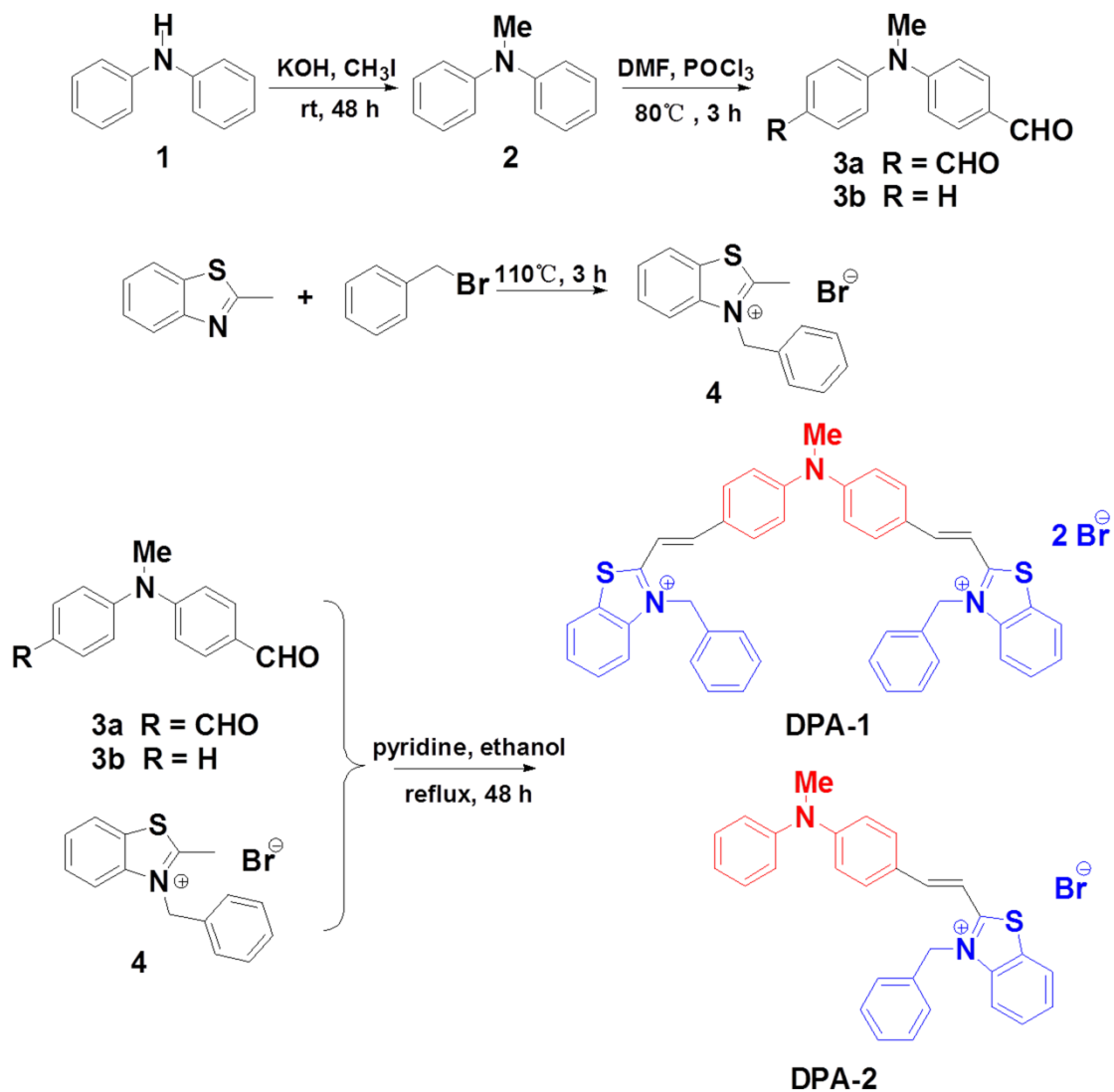
- activity and peroxynitrite synthesis in cholesterol-enriched endothelial-cell membranes *Biochem. Pharmacol.* 49 (1995) 1589-1600.
- [5] O. Nadiv, M. Shinitzky, H. Manu, D. Hecht, C. T. Roberts, D. Leroith, Y. Zick, Elevated protein tyrosine phosphatase activity and increased membrane viscosity are associated with impaired activation of the insulin receptor kinase in old rats, *Biochem. J.* 298 (1994) 443-450.
- [6] M. A. Haidekker, T. P. Brady, D. Lichlyter, E.A. Theodorakis, A ratiometric fluorescent viscosity sensor, *J. Am. Chem. Soc.* 128 (2006) 398-399.
- [7] M. A. Haidekker, E. A. Theodorakis, Molecular rotors--fluorescent biosensors for viscosity and flow, *Org. Biomol. Chem.* 5 (2007) 1669-1678.
- [8] J. Shao, S. Ji, X. Li, J. Zhao, F. Zhou, H. Guo, Thiophene-Inserted Aryl-Dicyanovinyl Compounds: The Second Generation of Fluorescent Molecular Rotors with Significantly Redshifted Emission and Large Stokes Shift, *Eur. J. Org. Chem.* 2011 (2011) 6100-6109.
- [9] F. Zhou, J. Shao, Y. Yang, J. Zhao, H. Guo, X. Li, S. Ji, Z. Zhang, Molecular Rotors as Fluorescent Viscosity Sensors: Molecular Design, Polarity Sensitivity, Dipole Moments Changes, Screening Solvents, and Deactivation Channel of the Excited States, *Eur. J. Org. Chem.* (2011) 4773-4787.
- [10] G. Y. Marina K. Kuimova, James A. Levitt, and Klaus Suhling., Molecular Rotor Measures Viscosity of Live Cells via Fluorescence Lifetime Imaging, *J. Am. Chem. Soc.* 130 (2008) 6672-6673.
- [11] M. A. Haidekker, T. P. Brady, S.H. Chalian, W. Akers, D. Lichlyter, E. A. Theodorakis, Hydrophilic molecular rotor derivatives - synthesis and characterization, *Bioorg. Chem.* 32 (2004) 274-289.
- [12] K. P. Ghiggino, J. A. Hutchison, S. J. Langford, M. J. Latter, M. A. P. Lee, P.R. Lowenstern, C. Scholes, M. Takezaki, B. E. Wilman, Porphyrin-Based Molecular Rotors as Fluorescent Probes of Nanoscale Environments, *Adv. Funct. Mater.* 17 (2007) 805-813.
- [13] J. Li, Y. Zhang, H. Zhang, X. Xuan, M. Xie, S. Xia, G. Qu, H. Guo, Nucleoside-Based Ultrasensitive Fluorescent Probe for the Dual-Mode Imaging of Microviscosity in Living Cells, *Anal. Chem.* 88 (2016) 5554-5560.
- [14] H. Zhu, J. Fan, M. Li, J. Cao, J. Wang, X. Peng, A "distorted-BODIPY"-based fluorescent probe for imaging of cellular viscosity in live cells, *Chem. Eur. J.* 20 (2014) 4691-4696.
- [15] Z. Yang, Y. He, J. H. Lee, N. Park, M. Suh, W. S. Chae, J. Cao, X. Peng, H. Jung, C. Kang, J. S. Kim, A self-calibrating bipartite viscosity sensor for mitochondria, *J. Am. Chem. Soc.* 135 (2013) 9181-9185.
- [16] L. Wang, Y. Xiao, W. Tian, L. Deng, Activatable rotor for quantifying lysosomal viscosity in living cells, *J. Am. Chem. Soc.* 135 (2013) 2903-2906.
- [17] R. Weissleder, A clearer vision for in vivo imaging, *Nat. Biotechnol.* 19 (2001) 316-317.
- [18] R. Weissleder, V. Ntziachristos, Shedding light onto live molecular targets, *Nat. Med.* 9 (2003) 123-128.
- [19] W. Sun, S. Guo, C. Hu, J. Fan, X. Peng, Recent Development of Chemosensors Based on Cyanine Platforms, *Chem. Rev.* 116 (2016) 7768-7817.
- [20] M. Wang, Y. Zhang, X. Yue, S. Yao, M.V. Bondar, K.D. Belfield, A Deoxyuridine-Based Far-Red Emitting Viscosity Sensor, *Molecules* 21 (2016).
- [21] X. Wang, F. Song, X. Peng, A versatile fluorescent probe for imaging viscosity and hypochlorite in living cells, *Dyes Pigm* 125 (2016) 89-94.

- [22] Y. Baek, S. J. Park, X. Zhou, G. Kim, H. M. Kim, J. Yoon, A viscosity sensitive fluorescent dye for real-time monitoring of mitochondria transport in neurons, *Biosens. Bioelectron.* 86 (2016) 885-891.
- [23] F. Liu, T. Wu, J. Cao, S. Cui, Z. Yang, X. Qiang, S. Sun, F. Song, J. Fan, J. Wang, X. Peng, Ratiometric detection of viscosity using a two-photon fluorescent sensor, *Chem. Eur. J.* 19 (2013) 1548-1553.
- [24] Y. Zhang, X. Yue, B. Kim, S. Yao, K.D. Belfield, Deoxyribonucleoside-modified squaraines as near-IR viscosity sensors, *Chem. Eur. J.* 20 (2014) 7249-7253.
- [25] X. J. Peng, F. L. Song, E. Lu, Y. N. Wang, W. Zhou, J. L. Fan, Y. L. Gao, Heptamethine cyanine dyes with a large stokes shift and strong fluorescence: A paradigm for excited-state intramolecular charge transfer, *J. Am. Chem. Soc.* 127 (2005) 4170-4171.
- [26] L. Fan, Y. J. Fu, Q. L. Liu, D. T. Lu, C. Dong, S. M. Shuang, Novel far-visible and near-infrared pH probes based on styrylcyanine for imaging intracellular pH in live cells, *Chem. Commun.* 48 (2012) 11202-11204.
- [27] H. Li, Q. Yao, J. Fan, J. Du, J. Wang, X. Peng, An NIR fluorescent probe of uric HSA for renal diseases warning, *Dyes Pigm* 133 (2016) 79-85.
- [28] R. D. Telore, N. Sekar, Carbazole-containing push-pull chromophore with viscosity and polarity sensitive emissions: Synthesis and photophysical properties, *Dyes Pigm* 129 (2016) 1-8.
- [29] Z. Liu, C. Zhang, W. He, F. Qian, X. Yang, X. Gao, Z. Guo, A charge transfer type pH responsive fluorescent probe and its intracellular application, *New J. Chem.* 34 (2010) 656.
- [30] A. Kovalchuk, J.L. Bricks, G. Reck, K. Rurack, B. Schulz, A. Szumna, H. Weisshoff, A charge transfer-type fluorescent molecular sensor that "lights up" in the visible upon hydrogen bond-assisted complexation of anions, *Chem. Commun.* (2004) 1946-1947.
- [31] B. Zhu, F. Yuan, R. Li, Y. Li, Q. Wei, Z. Ma, B. Du, X. Zhang, A highly selective colorimetric and ratiometric fluorescent chemodosimeter for imaging fluoride ions in living cells, *Chem. Commun.* 47 (2011) 7098-7100.
- [32] X. Chen, H. Li, L. Jin, B. Yin, A ratiometric fluorescent probe for palladium detection based on an allyl carbonate group functionalized hemicyanine dye, *Tetrahedron Lett.* 55 (2014) 2537-2540.
- [33] N. Jiang, J. Fan, F. Xu, X. Peng, H. Mu, J. Wang, X. Xiong, Ratiometric fluorescence imaging of cellular polarity: decrease in mitochondrial polarity in cancer cells, *Angew. Chem. Int. Ed. Engl.* 54 (2015) 2510-2514.
- [34] S. Tatay, P. Gavina, E. Coronado, E. Palomares, Optical mercury sensing using a benzothiazolium hemicyanine dye, *Org. Lett.* 8 (2006) 3857-3860.
- [35] K. C. Majumdar, B. Chattopadhyay, S. Chakravorty, N. Pal, R.K. Sinha, A new type of symmetrical banana-shaped material based on N-methyldiphenylamine as a core moiety exhibiting an Ad→A2 transition, *Tetrahedron Lett.* 49 (2008) 7149-7152.
- [36] X. Zhang, L. Chi, S. Ji, Y. Wu, P. Song, K. Han, H. Guo, T. D. James, and J. Zhao, Rational design of d-PeT phenylethynylated-carbazole monoboronic acid fluorescent sensors for the selective detection of r-hydroxyl carboxylic acids and monosaccharides, *J. Am. Chem. Soc.* 131 (2009) 17452-17463.
- [37] J. Y. S. Ji, Q. Yang, S. Liu, M. Chen, and J. Zhao, Tuning the intramolecular charge transfer of alkynylpyrenes: effect on photophysical properties and its application in design of OFF-ON

- fluorescent thiol probes, *J. Org. Chem.* 74 (2009) 4855-4865.
- [38] A. Latrofa, M. Franco, A. Lopodota, et al., Structural modifications and antimicrobial activity of N-cycloalkenyl-2-acylalkylidene-2,3-dihydro-1,3-benzothiazoles, *Farmaco* 60 (2005) 291-297.
- [39] A. C. Hernandez-Perez, S. K. Collins, A visible-light-mediated synthesis of carbazoles, *Angew. Chem. Int. Ed. Engl.* 52 (2013) 12696-12700.
- [40] H. H. T. Rance A. Velapoldi Corrected Emission Spectra and Quantum Yields for a Series of Fluorescent Compounds in the Visible Spectral Region, *J. Fluoresc* 14 (2004) 465-472.
- [41] T. Forster, G. Hoffmann, Viscosity dependence of fluorescent quantum yields of some dye systems, *Zeitschrift Fur Physikalische Chemie-Frankfurt* 75 (1971) 63-&.
- [42] T. G. Frisch MJ, Schlegel HB, Scuseria GE, Robb MA, Cheeseman JR, et al., Gaussian 09, revision C.01., Wallingford CT: Gaussian, Inc (2010).
- [43] A.D. Becke, Density-functional thermochemistry. III. The role of exact exchange, *J. Chem. Phys.* 98 (1993) 5648-5652.
- [44] W. J. H. R. Ditchfield, and J. A. Pople, Self-Consistent Molecular Orbital Methods. 9. Extended Gaussian-type basis for molecular-orbital studies of organic molecules, *J. Chem. Phys.* 54 (1971) 724.
- [45] K. B. J. P. Perdew, and M. Ernzerhof, Generalized gradient approximation made simple, *Phys. Rev. Lett.* 77 (1996) 3865-3868.
- [46] A. D. M. a. G. S. Chandler, Contracted Gaussian-basis sets for molecular calculations. 1. 2nd row atoms, Z=11-18, *J. Chem. Phys.* 72 (1980) 5639-5648.
- [47] Y. Zhang, K. Wang, G. Zhuang, Z. Xie, C. Zhang, F. Cao, G. Pan, H. Chen, B. Zou, Y. Ma, Multicolored-fluorescence switching of ICT-type organic solids with clear color difference: mechanically controlled excited state, *Chem. Eur. J.* 21 (2015) 2474-2479.
- [48] J. Cao, T. Wu, C. Hu, T. Liu, W. Sun, J. Fan, X. Peng, The nature of the different environmental sensitivity of symmetrical and unsymmetrical cyanine dyes: an experimental and theoretical study, *Phys. Chem. Chem. Phys.* 14 (2012) 13702-13708.
- [49] T. A. Oelkrug D, Gierschner J, Egelhaaf H, Hanack M, Hohloch M, et al., Tuning of fluorescence in films and nanoparticles of oligophenylenevinyls, *J. Phys. Chem. B* 102 (1998) 1902-1907.
- [50] A. Mishra, R.K. Behera, P. K. Behera, B.K. Mishra, G.B. Behera, Cyanines during the 1990s: A Review, *Chem. Rev.* 100 (2000) 1973-2012.
- [51] P. A. Hunt, M.A. Robb, Systematic control of photochemistry: The dynamics of photoisomerization of a model cyanine dye, *J. Am. Chem. Soc.* 127 (2005) 5720-5726.
- [52] G. L. Silva, V. Ediz, D. Yaron, B. A. Armitage, Experimental and computational investigation of unsymmetrical cyanine dyes: Understanding torsionally responsive fluorogenic dyes, *J. Am. Chem. Soc.* 129 (2007) 5710-5718.
- [53] M. Dekhtyar, W. Rettig, M. Sczepan, Small S-0-S-1 energy gaps for certain twisted conformations of unsymmetric polymethine dyes: quantum chemical treatment and spectroscopic manifestations, *Phys. Chem. Chem. Phys.* 2 (2000) 1129-1136.

Figure Caption

Styrylcyanine-based fluorescent probes with red-emission and large Stokes shift for the detection of viscosity



Scheme 1. Synthetic routes for **DPA-1** and **DPA-2**.

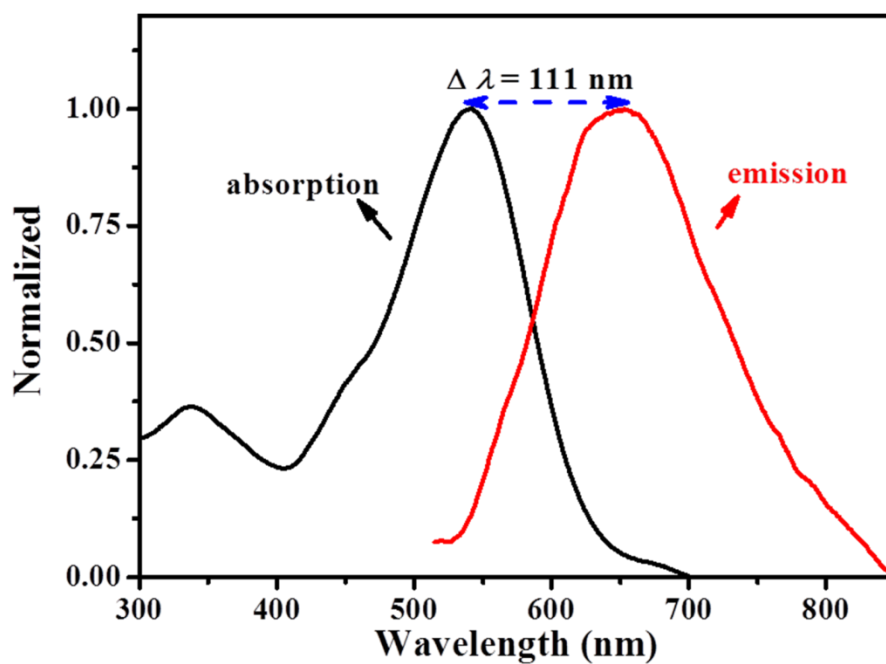


Fig. 1. Normalized absorption and emission spectra of **DPA-1** in water (containing 1% DMSO).

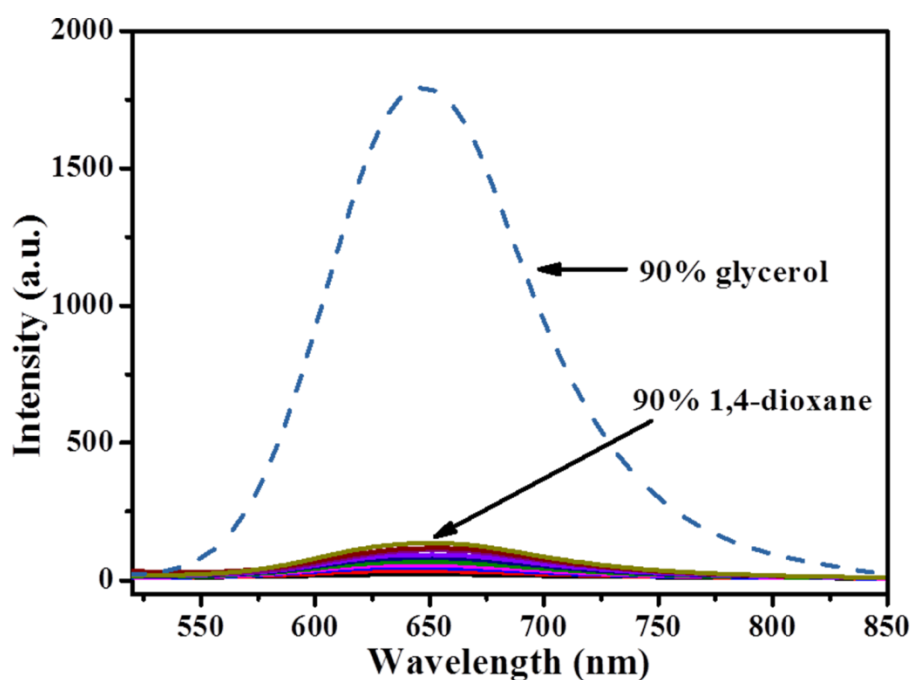
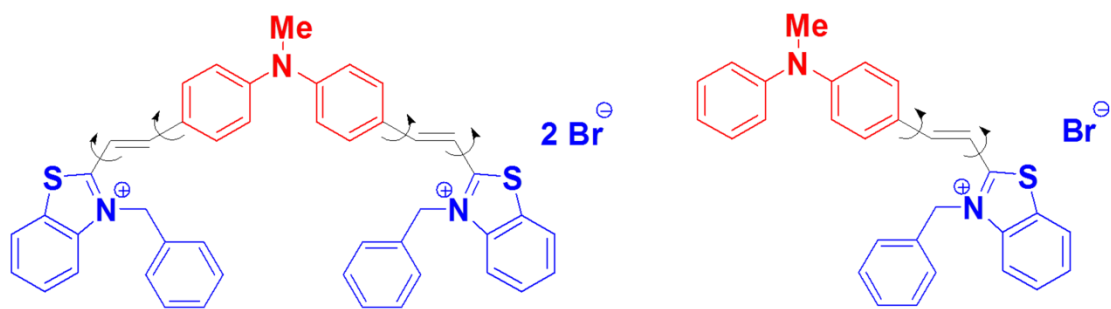


Fig. 2. The emission spectra of **DPA-1** (10 μ M) in different solution. The solid lines represent the probe in different proportional water and 1, 4-dioxane mixtures; the dash curve represents **DPA-1** in water-glycerol (10:90, v/v) under the same condition.



Scheme 2. Hypothetical rotation of the probes in low viscosity media.

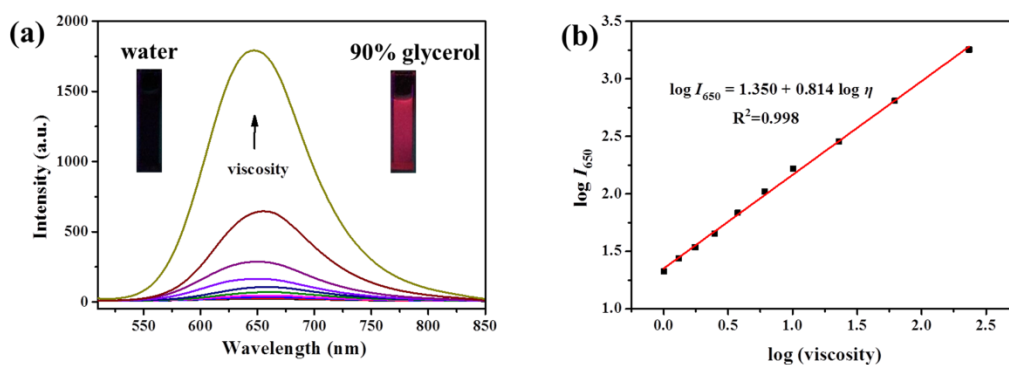


Fig. 3. (a) Fluorescence emission spectra of **DPA-1** (10 μM) in water and glycerol mixtures with different viscosity. Inset: the photographs of **DPA-1** in water (left) and 90% glycerol (right) under a 365 nm UV lamp. (b) The linear relationship between $\log I_{650}$ and $\log \eta$.

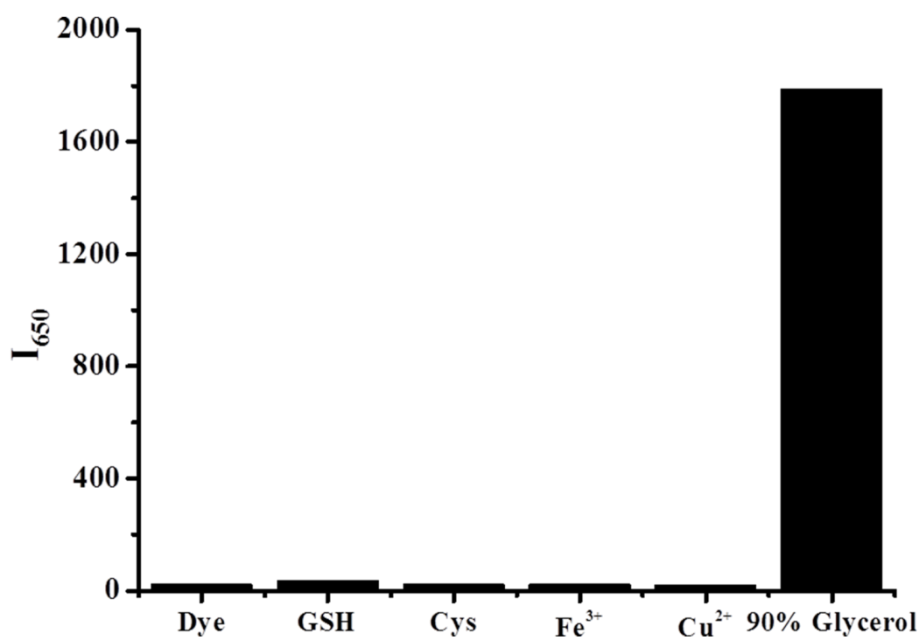


Fig. 4. The fluorescence spectra titration of **DPA-1** (10 μM) in water by GSH (1 mM); Cys (1 mM); Fe^{3+} (0.1 mM); Cu^{2+} (0.1 mM). Luminescence measurements were carried out three minutes after the addition of analytes at room temperature.

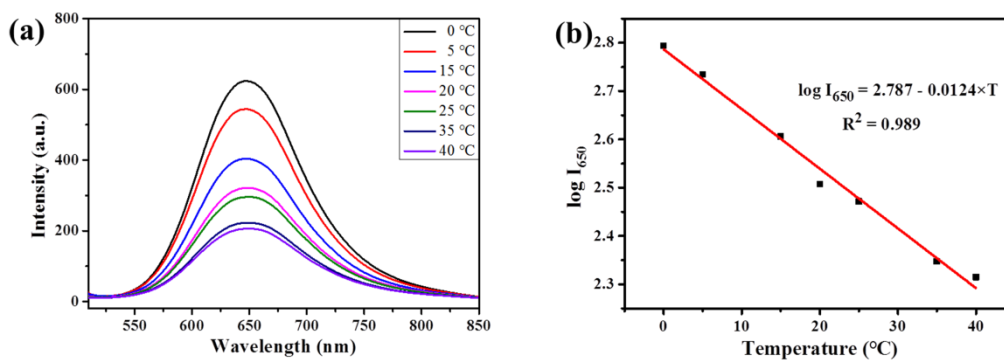


Fig. 5. (a) The fluorescence spectra of **DPA-1** (10 μM) at different temperatures in 70% glycerol. (b) Dependence between $\log I_{650}$ and temperature.

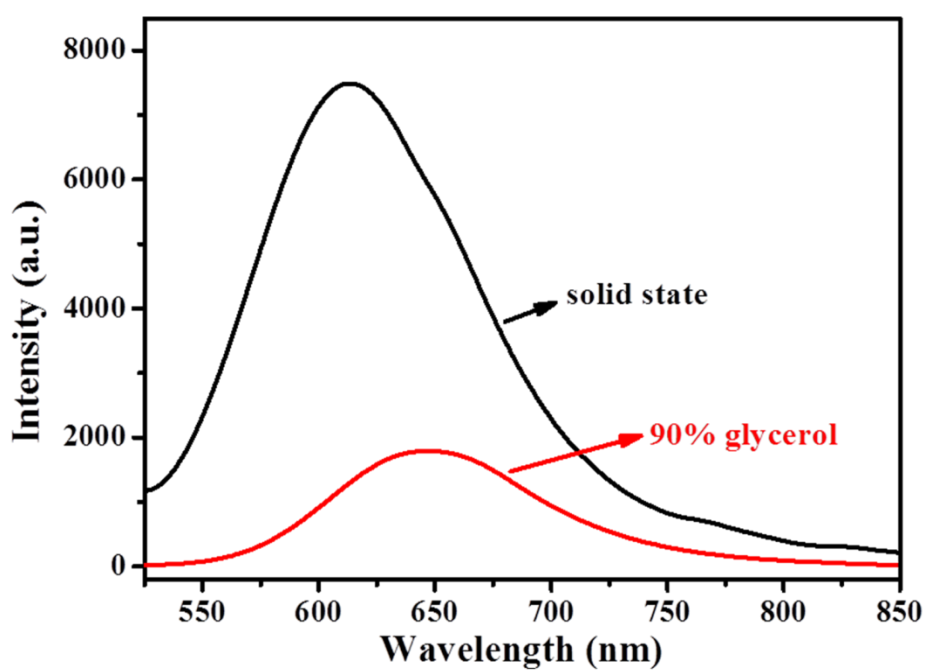


Fig. 6. (a) Fluorescence spectra of **DPA-1** in different states. The black color represents **DPA-1** in PMMA film; the red color in the figure is the dye in 90% glycerol (10 μM).

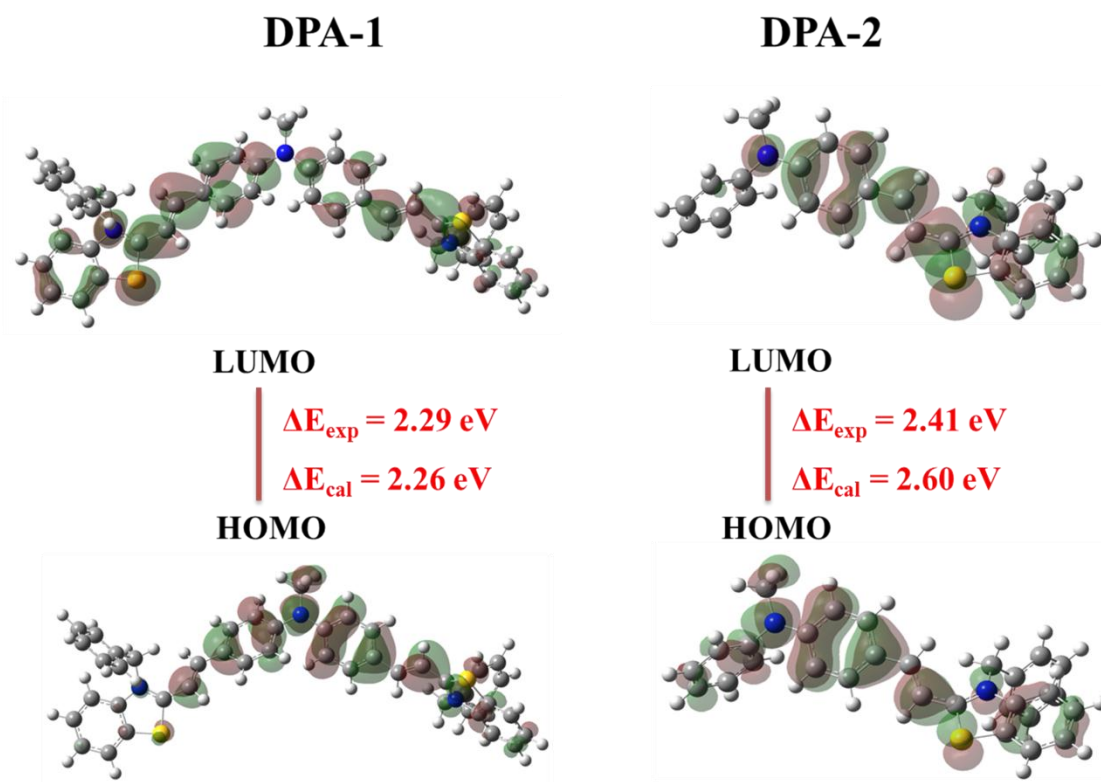
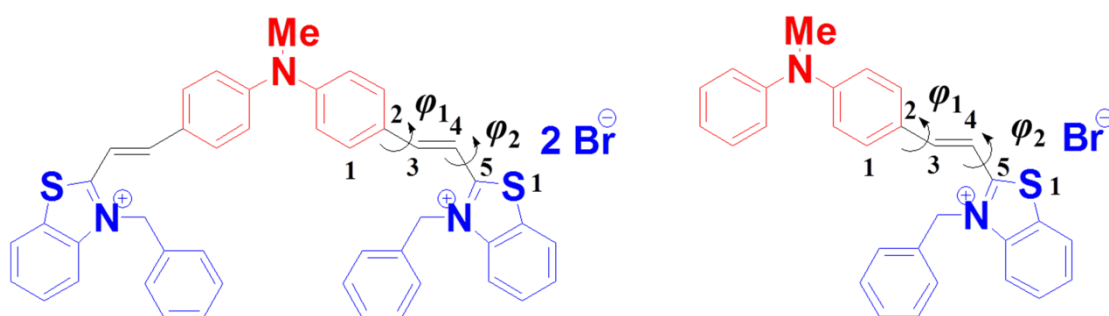


Fig. 7. Frontier molecular orbital profiles after geometry optimization of **DPA-1** and **DPA-2**, calculated at the DFT/B3-LYP/6-31G* level. Absorption spectra were studied at the TDDFT/PBE0/6-311G* level in water with IEFPCM model.



Scheme 3. Definition of angles, φ_1 and φ_2 , used to describe the rotation about different C-C bonds. φ_1 represents the dihedral angle of C1-C2-C3-C4 and φ_2 represents the dihedral angle of C3-C4-C5-S1.

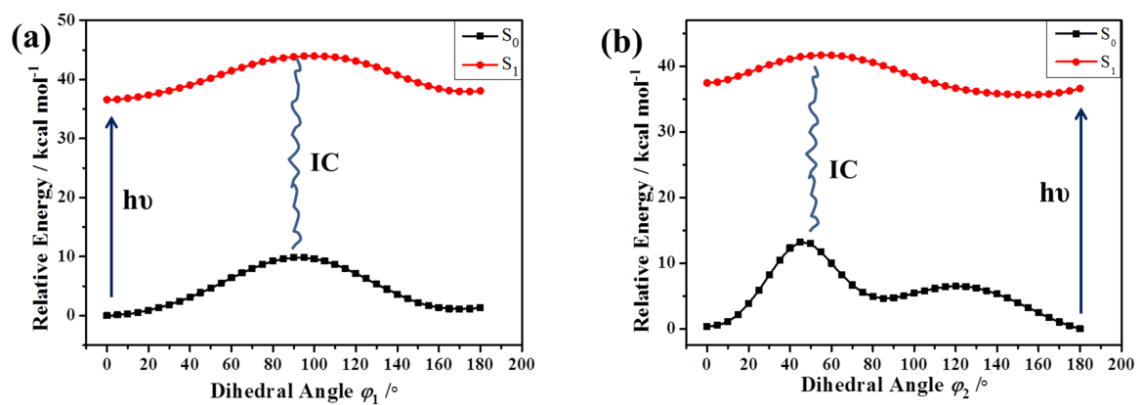


Fig. 8. Potential-energy curves of **DPA-1** at S₀ (black) and S₁ states (red) rotation along with chemical bond φ_1 (a) and chemical bond φ_2 (b), calculated at the TDDFT/B3-LYP/6-31G* level.

IC: internal conversion.

Styrylcyanine-based fluorescent probes with red-emission and large Stokes shift for the detection of viscosity

Table 1 Activation energies of S_1 and energy gaps between the S_0 and S_1 states rotation around different chemical bands (φ_1 and φ_2) for **DPA-1** and **DPA-2**.

Chemical bands	DPA-1		DPA-2	
	E_a (kcal mol ⁻¹)	E_{gap} (kcal mol ⁻¹)	E_a (kcal mol ⁻¹)	E_{gap} (kcal mol ⁻¹)
φ_1	7.26	34.01	15.67	17.22
φ_2	5.07	28.19	18.11	17.88